# Optical absorption of Ni-based alloys*

Madoka Tokumoto
*Electrotechnical Laboratory, 1-1-4 Umezono, Sakura-mura, Niihari-gun, Ibaraki, Japan*
(Received 11 February 1980)

A study of the optical absorption of Ni-based dilute alloys (*Ni*Co, *Ni*Fe, *Ni*V, *Ni*Ti) by a sensitive differential technique is presented. The experiment is analyzed for the difference in the optical conductivity between the alloy and pure Ni. The structures observed in the differential optical conductivity are classified into two groups; one is sensitive to impurity species and the other is not. The former is discussed in terms of the Friedel virtual-bound-state model of transition-metal-based dilute alloys. The latter is found to be described in terms of the electronic band structure of ferromagnetic nickel as arising from disorder-induced wave-vector-nonconserving optical-absorption processes. Based on these results we also present a reinterpretation of our previous *Ni*Cu data. The data appear to be consistent with the coherent-potential-approximation calculations of the density of states for Ni-rich alloys. Peaks at $\hbar\omega = 1$ eV (*Ni*Fe) and $\hbar\omega = 3$ eV (*Ni*Cu) are interpreted in terms of impurity density-of-states peaks 1 eV above, and 3 eV below the Fermi level, respectively.

## I. INTRODUCTION

The electronic structure of the Cu-Ni alloy series has been extensively studied both experimentally and theoretically. In Cu-rich alloys, the Ni-impurity $d$ levels lie in the $s$-$p$ bands and appear to be well described[1-3] by the virtual-bound-state model of Friedel[4] and Anderson.[5] In our previous paper,[6] we presented a study of the optical properties of Ni-rich Cu-Ni alloys. We showed that the differential optical conductivity of *Ni*Cu alloys provides a sensitive probe to the change of the electronic structure of Ni upon alloying. An interpretation of the optical data in terms of a contribution due to transitions from Cu-impurity levels to band states above the Fermi level, and a negative contribution corresponding to a reduction in the interband conductivity in the alloy was presented and shown to be consistent with the band-structure calculations for ferromagnetic nickel. However, from the data on the *Ni*Cu system alone, it was not possible to make a definitive interpretation. Since the host transition metal itself has a complex electronic structure throughout the spectral range of interest, the absorption due to impurity levels is superimposed on spectral features due to the changes in the electronic structure of the host metal upon alloying. The motivation for this study on Ni-based alloy series with different impurities is to more clearly identify these different features.

The present investigation of nickel-based 3$d$ transition-metal alloys was undertaken with two objectives in mind. Firstly, we wanted to study the differential optical conductivity spectrum as a function of the impurity potentials in order to clarify identifications of optical absorption associated with impurity states. Secondly, we wanted to find out if some of the structures in the differential optical conductivity could be described in terms of the band structure of host metal as arising from nonvertical transitions which are caused by disorder-induced relaxation of the conservation of crystal momentum. To our knowledge, no explicit evidence of such an impurity-induced indirect transition has been reported so far concerning the optical study of the transition-metal alloys.

The decision to study the nickel-based alloy system in preference to other 3$d$ transition-metal-based alloy systems was based on the following considerations. Since the $d$ bands of the ferromagnetic Ni lie almost entirely below the Fermi level with only the minority spin $d$ band extending a small fraction of an eV above the Fermi level, the final states in the absorption process lie either in the flat $s$-$p$ bands or in the very sharp minority spin $d$ band at the Fermi level. It is this simplicity of the final states of the absorption process that makes the nickel-based alloy system the first choice for the optical study.[7]

The paper is organized as follows. The experiment is described in Sec. II and the interpretation of the optical data on *Ni*Co, *Ni*Fe, *Ni*V, and *Ni*Ti alloys is discussed in Sec. III. In Sec. IV, we present reinterpretation of the optical data on *Ni*Cu alloys. Concluding remarks are made in Sec. V.

## II. EXPERIMENTAL

The samples were prepared by simultaneous vacuum evaporation of the two constituents onto polished fused quartz substrates. Two identical substrates were mounted in the evaporation chamber in a geometry such that one received

 

nickel only providing the pure comparison sample, while the other substrate received both constituents. The nickel was evaporated with an electron-beam evaporation source, while another solute metal constituent was evaporated from a tungsten boat by resistive heating. The concentrations of the alloy samples were determined from the ratio of the deposition rates of the two constituents, monitored separately with two calibrated quartz oscillators. Details of sample preparation and other experimental conditions were described elsewhere.[6]

We have used a single-beam differential reflectance technique, similar to that described by Beaglehole,[8] in order to measure the change in reflectivity of the pure nickel with the addition of small amounts of other $3d$ transition metals. Both pure and alloy samples were mounted on a rotating holder so that light was reflected alternatively from a pure sample and an alloy sample. The quantity, related to the difference in reflectivity $\alpha \equiv (R_{\text{pure}} - R_{\text{alloy}})/(R_{\text{pure}} + R_{\text{alloy}})$, was recorded continuously as a function of photon wavelength. In Fig. 1, $\alpha$ is shown for representative samples of *Ni*Co, *Ni*Fe, *Ni*V, and *Ni*Ti alloys with concentrations around 4 at. %.

The complex conductivity function $\hat{\sigma} = \sigma_1 + i\sigma_2$ of the sample was obtained through a Kramers-Kronig analysis of the reflectivity data. The reflectivity of the pure-nickel films was measured separately using a Perkin-Elmer model 350 spectrophotometer with a specular reflectance accessory. The phase shift $\theta(\omega)$ of the complex reflectivity $\hat{r}(\omega) = [R(\omega)]^{1/2} e^{i\theta(\omega)}$ was obtained from the near-normal-incidence reflectivity data with the aid of the phase-shift dispersion relation

$$\theta(\omega) = \frac{\omega}{\pi} P \int_0^\infty \frac{\ln R(\omega)}{\omega^2 - \omega'^2} d\omega' . \tag{1}$$

After $\theta(\omega)$ is obtained, the complex dielectric function $\hat{\epsilon}(\omega)$ is computed from Fresnel's relation

$$\hat{\epsilon}(\omega) = \left(\frac{1 + \hat{r}(\omega)}{1 - \hat{r}(\omega)}\right)^2 , \tag{2}$$

and the complex conductivity function $\hat{\sigma}(\omega)$ is computed from

$$\hat{\sigma}(\omega) = \frac{\omega}{4\pi i} [\hat{\epsilon}(\omega) - 1] . \tag{3}$$

$\hat{\sigma}^{\text{pure}}$ and $\hat{\sigma}^{\text{alloy}}$ were obtained separately from $R_{\text{pure}}$ and $R_{\text{alloy}} = R_{\text{pure}}[(1-\alpha)/(1+\alpha)]$. The results were then presented in terms of the differential conductivity $\Delta\sigma_1 = \sigma_1^{\text{alloy}} - \sigma_1^{\text{pure}}$. In order to perform the Kramers-Kronig analysis, it was necessary to extrapolate the reflectivity data outside the measured spectral range. Both low- and high-energy extrapolations were made following the procedure described in our previous paper on *Ni*Cu alloy.[6] The differential conductivity is not very sensitive to the details of the extrapolation.

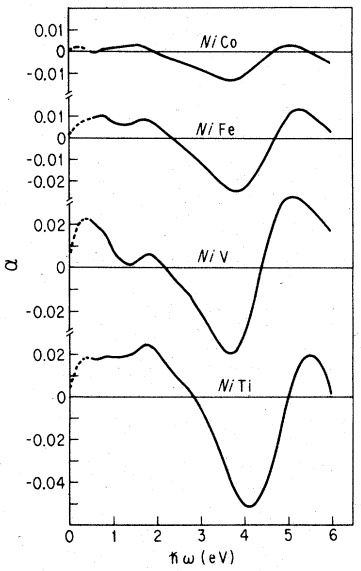


FIG. 1. Experimental curves of the differential reflectivity $\alpha = (R_{\text{pure}} - R_{\text{alloy}})/(R_{\text{pure}} + R_{\text{alloy}})$ for *Ni*Co, *Ni*Fe, *Ni*V, and *Ni*Ti alloy films. Alloy concentrations are about 4 at. %.

## III. DISCUSSION

The results for $\Delta\sigma_1$ for *Ni*Co, *Ni*Fe, *Ni*V, and *Ni*Ti are shown in Fig. 2. We will be discussing the following spectral features in this section. The low-frequency part (below 1.5 eV) contains a sharply rising low-frequency divergence in common, except for *Ni*Fe where a pronounced peak is observed around 1 eV. The second feature of interest is a peak around 2 eV which is commonly seen for all four kinds of alloys with different impurity species. Finally, at higher frequencies, there is a structure that appears to be related to the 4.5-eV peak in the conductivity of pure Ni.

We will discuss the interpretation of the $\Delta\sigma_1$ spectra in terms of three processes: (a) Modifications in the host density of states which can include a reduction due to the replacement of host atoms with the impurity atoms and shifts and broadening of host bands. (b) Absorption associated with the impurity density of states. This includes transitions from host states to empty impurity states as well as transitions from impurity states to host states. (c) Impurity-induced indirect transitions (wave-vector-nonconserving transitions). In this process it is expected that optical-absorption edges can occur at frequencies corresponding to the separation of peaks in the host density of states and the Fermi level, and

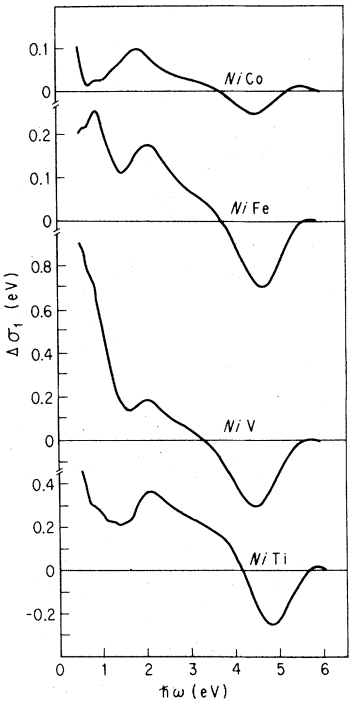


FIG. 2. The differential optical conductivity $\Delta\sigma_1 = \sigma_1^{\text{alloy}} - \sigma_1^{\text{pure}}$ obtained by Kramers-Kronig analysis of data in Fig. 1.

optical-absorption peaks can occur at frequencies corresponding to the separation of occupied and unoccupied peaks in the host density of states.

Of these three processes, (a) and (b) have been considered by Beaglehole and Hendrickson[9] in analyzing and interpreting their reflectivity data from dilute *Au*Fe alloys. From a theoretical standpoint, only process (b) has been usefully developed in the literature. Several authors[10-12] have considered the optical response within the Anderson model[5] of dilute alloys. They have only considered the case where the impurity is placed in a simple free-electron-like band. Since the final states of the absorption process in ferromagnetic Ni-rich alloys would be either the free-electron-like *s-p* bands above the Fermi level or the empty part of the minority *d* band, these calculations are applicable except for transitions whose final state is the sharp density-of-states peak at the top of the minority *d* band.

Process (c) has been considered by Joesten and Brown[13] in analyzing and interpreting their optical absorption data from AgCl-AgBr mixed crystals. Since AgCl and AgBr are both indirect band-gap materials, long-wavelength absorption tails arise from phonon-assisted indirect transitions. In AgBr-rich mixed crystals of AgCl and AgBr, an additional absorption appeared at an energy precisely halfway between the indirect phonon-emission and phonon-absorption thresholds. This disorder-induced zero-phonon absorption was described in terms of the pure-crystal band structure as arising from transitions which are nonvertical since different points of the Brillouin zone were involved. A similar change in the selection rule for phonon wave vector occurs in infrared absorption and Raman scattering, and defect-activated infrared absorption (DAIA)[14] and defect-activated first-order Raman scattering (DARS)[15] have been observed. No experimental evidence of process (c) has been reported so far on optical study of transition-metal-based alloys. Theoretical aspects of process (c) in alloys have recently been developed by Parlebas and Mills.[16,17]

We will first take up the features seen commonly in our $\Delta\sigma_1$ spectra and interpret them in terms of processes (a) and (c) which we suppose are rather insensitive to the species of impurity atoms. We will consider later how remaining structures can be explained in terms of process (b).

The $\Delta\sigma_1$ peak at about 2 eV and the $\Delta\sigma_1$ dip around 4.5 eV are commonly seen for all four alloys with different impurities. In process (a) we expect close correlation between structures in $\Delta\sigma_1$ and those in the optical conductivity of pure Ni, $\sigma_1^{\text{pure}}$. The $\sigma_1^{\text{pure}}$ [Fig. 4(a)] is smooth compared with our $\Delta\sigma_1$ spectra (Fig. 2). The most notable structure in $\sigma_1^{\text{pure}}$ is the peak at 4.5 eV. Therefore, we expect a negative contribution to $\Delta\sigma_1$ as discussed in (a) that should be smooth except near 4.5 eV. In the simplest model this contribution would go like $\Delta\sigma_1 \sim -c\sigma_1^{\text{pure}}$, where $c$ is the concentration of solute atoms. *Anticorrelation* between $\Delta\sigma_1$ and $\sigma_1^{\text{pure}}$ around 4.5 eV supports our interpretation that the 4.5-eV dip in $\Delta\sigma_1$ is caused by process (a).

The 2 eV peak in $\Delta\sigma_1$ must have a different origin since $\sigma_1^{\text{pure}}$ is smooth and structureless around 2 eV. One possible interpretation is to associate this structure with optical transition between two prominent peaks in the minority spin band density of states. (See Fig. 3) Since this transition involves the Fermi level, one might be tempted to interpret this peak in terms of the rigid-band model as arising from increased *d* holes as a result of introduction of impurities with smaller atomic number. This possibility is excluded by the fact that $\Delta\sigma_1$ in *Ni*Cu alloys also has a peak at 2 eV instead of a dip which the rigid-band model would predict since Cu would introduce an additional electron and fill the *d* holes.

We want to see if this peak is consistent with the host electronic density of state through process (c). While Parlebas and Mills[16,17] gave a theoretical basis for the possibility of observing structures

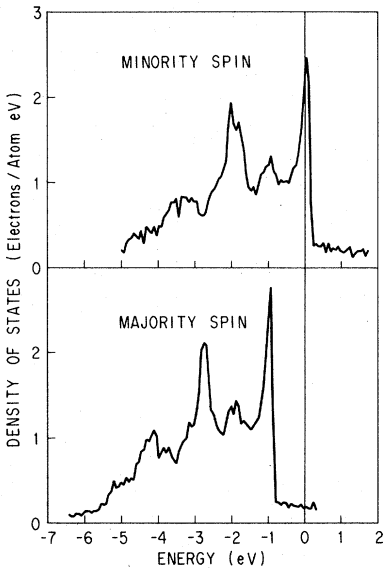


FIG. 3. Electron density of states for majority and minority spins of ferromagnetic Ni, from Ref. 18. The energy is measured with respect to the Fermi level.

related to process (c) in optical spectra of alloys, their model calculations are not in a form that can be readily compared with our experimental results. In order to gain some insight into the effect of process (c), we have made the following simple calculation of the optical conductivity for the case of ferromagnetic Ni.

If we completely ignore wave-vector conservation and take a constant transition matrix element, we obtain a simple result for the optical conductivity which we will refer to as the indirect model. In the indirect model, the interband part of the optical conductivity is found from the density of states as

$$\sigma_1(\omega) \propto \frac{1}{\omega} \int_{E_F}^{E_F+\hbar\omega} n_f(E) n_i(E-\hbar\omega) dE \,. \tag{4}$$

Here $n_i$ and $n_f$ refer to initial- and final-state densities below and above the Fermi level, respectively. For the present calculation, the density of states for the majority and minority spins are taken from the ferromagnetic Ni band-structure calculation by Connolly[18] (Fig. 3). With spin-orbit coupling ignored, the evaluation of this integral for the majority and minority spin band structure of Ni is made separately as shown in Fig. 4(a), together with the sum of the two. The majority spin conductivity $\sigma_1^{maj}$ shows an edge around 1 eV, which is associated with an onset of optical transition from the top of the majority $d$ band. The minority spin conductivity $\sigma_1^{min}$ shows a sharply rising low-frequency divergence below 1 eV, a shoulder at 1 eV, and a prominent peak around

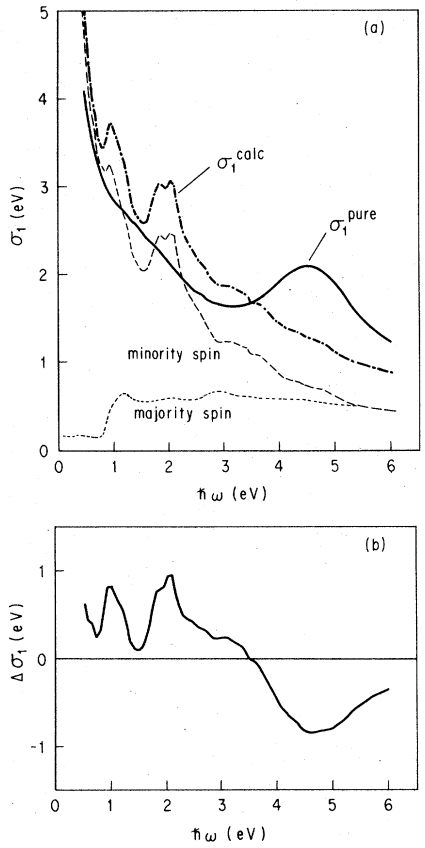


FIG. 4. (a) Optical conductivity for Ni calculated assuming non-$k$-conserving transitions. The dash-dot line $\sigma_1^{calc}$ is the sum of contributions from majority and minority spin bands. The measured optical conductivity $\sigma_1^{pure}$, which is considered to result mainly from $k$-conserving transitions, is shown as a solid line. The difference between these curves is related to the change in absorption spectra produced by the introduction of disorder in alloys. (b) Calculated differential optical conductivity $\Delta\sigma_1 = \sigma_1^{calc} - \sigma_1^{pure}$ showing a possible contribution from the disorder-induced wave-vector-nonconserving absorption.

2 eV. The experimentally observed low-frequency divergence of $\sigma_1^{pure}$ can thus be explained in this model by interband transitions within the minority spin band, with a relatively small contribution from a Drude-type absorption. A shoulder at 1 eV originates in transitions from a small $e_g$ peak in the middle of two prominent $t_{2g}$ peaks. A peak around 2 eV is caused by transitions from the lower $t_{2g}$ peak in the middle of the minority $d$ band to the sharp $t_{2g}$ peak at the Fermi level. In the total conductivity $\sigma_1^{calc}$ ($= \sigma_1^{maj} + \sigma_1^{min}$), in addition to the 2 eV peak originating in $\sigma_1^{min}$, a new peak is formed at about 1 eV out of an edge in $\sigma_1^{maj}$ and a shoulder in $\sigma_1^{min}$. Since constant matrix elements are used, the scaling of the theoretical curve is,

of course, arbitrary. However, the conductivity sum rule gave us a proper scaling factor as shown in the figure. The experimental $\sigma_1^{pure}$ is also included in the figure for comparison. The indirect model completely neglects the wave-vector-conservation selection rule, while the actually observed $\sigma_1^{pure}$ is governed by the selection rule. We therefore expect that the difference between this theoretical calculation ($\sigma_1^{calc}$) and the experimental observation ($\sigma_1^{pure}$) would suggest how and to what extent the optical conductivity could change when the selection rule is relaxed upon introduction of impurities.[19] The difference $\Delta\sigma_1 = \sigma_1^{calc} - \sigma_1^{pure}$ is shown in Fig. 4(b). $\Delta\sigma_1$ in Fig. 4(b) has peaks at 1 and 2 eV and a dip around 4.5 eV. Upon comparison of Fig. 4(b) with Fig. 2, one clearly sees that the origin of the experimental $\Delta\sigma_1$ peak abound 2 eV can be interpreted in terms of process (c). Interestingly, the calculated $\Delta\sigma_1$ seems to fit to the experiment more than we expected. For example, a dip around 4.5 eV, which we attributed to process (a), can also be explained by this model in terms of process (c). This suggests that the processes (a) and (c) are not entirely independent. Indeed, optical absorption measures a transition density of states (TDOS) for which the total oscillator strength of the transition is conserved. Hence nondirect transitions allowed by process (c) would be expected to occur at the expense of prominent structures in the wave-vector-conserving TDOS of the pure metal. This effect is indistinguishable in optical studies from a reduction in the DOS mentioned in process (a). In this paper, however, we practically classified into process (a) only those cases where obvious *anti-correlation* between $\Delta\sigma_1$ and $\sigma_1^{pure}$ were observed.

A small but always observed shoulder at 0.9 eV can also be associated with process (c), although we can not identify the spin band from which it originates.

So far, we have been concerned with $\Delta\sigma_1$ structures which are commonly seen in different Ni-based alloys. This discussion shows that the common features in measured optical properties of the Ni-based alloys can be reasonably explained in terms of a model including process (a) and (c).

What about the optical absorption associated with the impurity density of states? This process (b) is expected to be fairly sensitive to the impurity species since the location of impurity levels in alloys such as *Ni*Co, *Ni*Fe, *Ni*Mn, etc., depends on the perturbing potential which is the difference of two terms: (1) a repulsive Coulomb term due to the decrease in nuclear charge and (2) an attractive exchange term due to the local increase in magnetic moment.[20]

A $\Delta\sigma_1$ peak at 1 eV for *Ni*Fe alloy is so pronounced that we consider the structure unique to Fe impurity and assign it to transitions of process (b). Several authors have studied impurity states in ferromagnetic nickel with more or less realistic density of states of the host metal.[20-23] Friedel[20] has shown that in strong ferromagnetic nickel-based alloys with 3*d* transition-metal impurities (*Ni*Mn, *Ni*Cr, *Ni*V), the virtual bound state can be pushed through the Fermi level when the repulsive impurity potential is strong enough. Indeed coherent-potential-approximation (CPA) calculations on *Ni*Fe alloys by Hasegawa and Kanamori[24] indicate formation of an empty impurity state of Fe about 1 eV above the Fermi level for the *minority* spin band of ferromagnetic Ni. In the CPA calculation, the minority spin band deforms to a considerable extent for a small concentration of Fe, whereas the majority spin band keeps the original shape approximately. We therefore interpret the $\Delta\sigma_1$ peak at 1 eV for *Ni*Fe alloy as being associated with transitions whose final state is a virtual bound state of Fe impurity atoms formed about 1 eV above the Fermi level. Virtual bound states in other alloys appear much less clear than in *Ni*Fe. In *Ni*Co, it would lie much closer to $E_F$ than in *Ni*Fe and would probably be out of our experimental range.[25] In *Ni*V, $\Delta\sigma_1$ shows a large low-energy divergence, and we may be observing a tail of virtual bound state associated with the majority and/or minority spin *d* band of Ni. In the CPA calculation,[24,25] the effective potential for one spin band at an impurity site strongly depends on the average density of electrons with opposite spin at the same site. Consequently, in contrast to Friedel's picture,[20] (i) the effective potentials for the majority and minority spin bands are usually quite different from each other, and (ii) they do not correlate with the original potential of impurity atoms in a simple manner. Similar CPA calculations on *Ni*V and *Ni*Ti would be helpful to make the interpretation clearer. Although the above interpretation is not unique, further optical studies on *Ni*Mn and *Ni*Cr alloys would be of great interest in connection with this model. It is to be noted that in spite of the wide acceptance of the concept of virtual-bound-state formation above the Fermi level in Ni-based 3*d* transition-metal alloys, no direct evidence of such empty states has been reported. Since photoelectron spectroscopy is ineffective for the study of these empty states, optical measurement, which gives information of the joint density of states, and appearance potential spectroscopy (APS), which gives the self-convolution of empty states, would be two of the most feasible candidates capable of direct observation of these virtual bound states above the Fermi level.

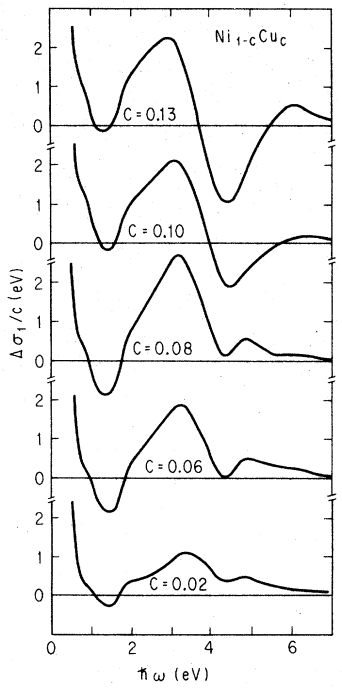


FIG. 5. The differential optical conductivity per atomic percent for a series of *Ni*Cu alloys.

## IV. REINTERPRETATION OF *Ni*Cu DATA

We present here a reinterpretation of our reflectivity data for the *Ni*Cu system, in light of the results of the present investigation on Ni-based alloy series. The results for $\Delta\sigma_1$ for *Ni*Cu alloys are taken from our previous paper[6] and reproduced in Fig. 5. The following spectral features were observed: (1) a low-frequency divergence below 1 eV and a shoulder at 0.9 eV, (2) a broad peak from 1.7 to 3 eV, and (3) a dip around 4.5 eV. Of these three features, the 4.5-eV dip was unambiguously assigned to process (a), i.e., reduction. The $\Delta\sigma_1$ structure from 1.7 to 3 eV was decomposed into double peaks and interpreted in terms of process (b) as arising from transitions from spin-split *d* levels of Cu impurities. This interpretation was plausible since nickel-rich Cu-Ni alloys are ferromagnetic at room temperature. However, the observed splitting appears to be too large if the 0.3-eV splitting measured by photoemission[26] is correct.

Now that the $\Delta\sigma_1$ peak at 2 eV is found to be insensitive to impurity species, we want to reinterpret these data as follows. $\Delta\sigma_1$ structure from 1.7 to 3 eV consists of two peaks, one at 2 eV and the other at about 3 eV. We now interpret these double peaks as having two different origins. The 3-eV peak is assigned to process (b) arising from transitions from Cu *d* states formed at about 3 eV below the Fermi level. This position of Cu *d* levels seems reasonable since Cu impurity acts as a weak but attractive potential in Ni. It is expected that Cu *d* levels in Ni are not sharp virtual levels since they fall within the high density of states of the *d* band of the host. Indeed, coherent-potential-approximation (CPA) calculations on low Cu concentration paramagnetic *Ni*Cu alloys by Stocks, Williams, and Faulkner[27] indicate a broad Cu density of states centered at about 4 eV below the Fermi level and with a half-width of more than 1 eV. Owing to the presence of the pronounced 4.5-eV dip, we cannot eliminate the possibility that Cu *d* states are much broader and extend down to 4 or 5 eV below the Fermi level.

The 2-eV peak and 0.9-eV shoulder can be interpreted in terms of impurity-induced wave-vector-nonconserving transitions, as discussed in Sec. III. In the present interpretation, it is unnecessary to consider the exchange splitting of Cu *d* levels in Ni-rich alloys, since we are not observing double peaks associated with transitions from impurity states to host states.

Spectral features of $\Delta\sigma_1$ for Ni-based alloys as assigned in Secs. III and IV are summarized in Table I.

TABLE I. Energies, characteristics, and identification of $\Delta\sigma_1$ structures in Ni-based alloys.

| Energy (eV) | Structure in $\Delta\sigma_1$ | Impurity dependence | Anticorrelation with $\sigma_1^{\text{pure}}$ | Origin |
|---|---|---|---|---|
| 0.9 | shoulder | No | No | (c) wave-vector-nonconserving transition |
| 1.0 | peak | Yes | No | (b) virtual bound state (Fe in Ni) |
| 2.0 | peak | No | No | (c) wave-vector-nonconserving transition |
| 3.0 | peak | Yes | No | (b) Cu *d* level |
| 4.5 | dip | No | Yes | (a) host reduction |

## V. CONCLUSIONS

We have shown that the differential optical conductivity of Ni-based alloys provides a sensitive probe to measure the change of electronic structure of Ni upon alloying. The structures observed in the differential optical conductivity can be classified into two groups, one is sensitive to the impurity species and the other is not. A calculation of optical conductivity based on the indirect model strongly supports the interpretation that some of the impurity-independent structures in the differential optical conductivity are caused by impurity-induced wave-vector-nonconserving transitions. This is the first experimental evidence to show that wave-vector-nonconserving process plays an important role in the optical properties of transition-metal-based alloys. This impurity-induced absorption component should be found in other alloy systems where the host electronic density of states have both occupied and unoccupied peaks involving different points of the Brillouin zone.

The remaining impurity-dependent structures can be interpreted in terms of the Friedel virtual-bound-state model as arising from transitions involving impurity $d$ states. This interpretation is consistent with the coherent-potential-approximation calculations for Ni-rich alloys. Studies of related alloys, such as $Ni$Mn and $Ni$Cr and those of Pd and Pt host with other transition- and noble-metal impurities, would lead to interesting new results and a more comprehensive understanding of the optical properties of transition-metal-based alloys.

## ACKNOWLEDGMENTS

The author would like to acknowledge useful discussions with several of our colleagues. First he wishes to express special thanks to H. D. Drew for the kind hospitality at the University of Maryland where we studied $Ni$Cu alloys, and for his helpful criticisms of this manuscript. He also thanks D. L. Mills for emphasizing the importance of the wave-vector-nonconserving processes in the interpretation of our previous study on the $Ni$Cu system, which motivated the present study. He acknowledges useful discussions with A. Bagchi, H. Sumi, S. Ogawa, and S. Wakoh. He has profited greatly from discussions with J. Kondo on aspects of this problem and critical reading of the manuscript. Finally, he wishes to thank T. Ishiguro and K. Kajimura for helpful discussions and support.

---

*This work was performed in part at the University of Maryland.

[1]H. D. Drew and R. E. Doezema, Phys. Rev. Lett. 28, 1581 (1972).

[2]B. Y. Lao, R. E. Doezema, and H. D. Drew, Solid State Commun. 15, 1253 (1974).

[3]D. Beaglehole, Phys. Rev. B 14, 341 (1976).

[4]J. Friedel, Nuovo Cimento Suppl. 2, 287 (1958).

[5]P. W. Anderson, Phys. Rev. 124, 41 (1961).

[6]M. Tokumoto, H. D. Drew, and A. Bagchi, Phys. Rev. B 16, 3497 (1977).

[7]Almost parallel argument applies to Pd- and Pt-based alloys with similar band structure, except that in these alloys $4d$ and $5d$ electrons, respectively, form the uppermost $d$ band and the exchange interaction is not strong enough to keep them ferromagnetic.

[8]D. Beaglehole, Appl. Opt. 7, 2218 (1968).

[9]D. Beaglehole and T. J. Hendrickson, Phys. Rev. Lett. 22, 133 (1969).

[10]B. Caroli, Phys. Kondens. Mater. 1, 346 (1963).

[11]B. Kjollerstrom, Philos. Mag. 19, 1207 (1969).

[12]A. J. Bennett and D. Penn, Phys. Rev. B 11, 3644 (1975).

[13]B. L. Joesten and F. C. Brown, Phys. Rev. 148, 919 (1966).

[14]M. Lax and E. Burstein, Phys. Rev. 97, 39 (1955).

[15]S. Ushioda, Solid State Commun. 15, 149 (1974).

[16]J. C. Parlebas and D. L. Mills, Phys. Rev. B 17, 3853 (1978).

[17]J. C. Parlebas and D. L. Mills, Phys. Rev. B 18, 3988 (1978).

[18]J. W. D. Connolly, Phys. Rev. 159, 415 (1967). We adopted Connolly's density of states instead of apparently more extensive work by Callaway and co-workers, simply because we do not need very fine structures of the density of states for the present study. The former is much simpler than the latter and still includes essential features characteristic to ferromagnetic Ni.

[19]Unfortunately, attempts to calculate the optical conductivity including the wave-vector conservation and wave-vector-dependent matrix elements do not successfully reproduce the measured optical conductivity of Ni. [See, for example, C. S. Wang and J. Callaway, Phys. Rev. B 9, 4897 (1974).] However, we believe at least the one-electron energy-band calculations are reliable. The indirect model should give a good reference for the case of relaxed wave-vector conservation so far as the density of states is correct.

[20]J. Friedel, in *Proceedings of the International School of Physics "Enrico Fermi" Course 37, Theory of Magnetism in Transition Metals*, edited by W. Marshall (Academic, New York, 1967).

[21]J. Kanamori, J. Appl. Phys. 36, 929 (1965).

[22]H. Hayakawa, Prog. Theor. Phys. 37, 213 (1967).

[23]H. Hayakawa and J. Yamashita, Prog. Theor. Phys. 54, 952 (1975).

[24]H. Hasegawa and J. Kanamori, J. Phys. Soc. Jpn. 31, 382 (1971).

[25]H. Hasegawa and J. Kanamori, J. Phys. Soc. Jpn. 33, 1599 (1972).

[26]D. E. Eastman, F. J. Himpsel, and J. A. Knapp, Phys. Rev. Lett. 40, 1514 (1978).

[27]G. M. Stocks, R. S. Williams, and J. S. Faulkner, Phys. Rev. B 4, 4390 (1971).